Function Based Isolation Forest (FuBIF): A Unifying Framework for Interpretable Isolation-Based Anomaly Detection

Alessio Arcudi * Alessandro Ferreri ** Francesco Borsatti ***
Gian Antonio Susto ***

- * Brain, Mind and Computer Science, University of Padova, Italy (e-mail: alessio.arcudi@phd.unipd.it)
- ** Department of Mathematics, Sapienza University of Roma, Italy (e-mail: alessandro.ferreri@uniroma1.it)
- *** Department of Information Engineering, University of Padova, Italy (e-mail: francesco.borsatti.1@phd.unipd.it, gianantonio.susto@unipd.it)

Abstract: Anomaly Detection (AD) is evolving through algorithms capable of identifying outliers in complex datasets. The Isolation Forest (IF), a pivotal AD technique, exhibits adaptability limitations and biases. This paper introduces the Function-based Isolation Forest (FuBIF), a generalization of IF that enables the use of real-valued functions for dataset branching, significantly enhancing the flexibility of evaluation tree construction. Complementing this, the FuBIF Feature Importance (FuBIFFI) algorithm extends the interpretability in IF-based approaches by providing feature importance scores across possible FuBIF models. This paper details the operational framework of FuBIF, evaluates its performance against established methods, and explores its theoretical contributions. An open-source implementation ¹ is provided to encourage further research and ensure reproducibility.

Keywords: Anomaly detection, Isolation forest, Explainable AI, Feature Importance

1. INTRODUCTION

The Isolation Forest (IF) of Liu et al. (2008) is a staple of anomaly detection, valued for its speed, frugal memory, and robust performance across speech, finance, and industrial monitoring tasks (Ounacer et al., 2018; Wu and Chen, 2018; Kabir et al., 2023). Yet IF's axis-parallel splits can bias scores whenever the relevant signal lies off the coordinate axes, prompting hypersphere, extended, and generalized variants that bend or rotate the decision surface (Hariri et al., 2019; Choudhury et al., 2021; Lesouple et al., 2021; Xu et al., 2022). Almost all of these advances postpone *interpretability*, yielding patchy, method-specific heuristics that hamper root-cause analysis.

We close both gaps with Function-Based Isolation Forest (FuBIF) and its explanation layer, FuBIFFI.

1 repository: https://github.com/anonymous2532/FuBIF

Each tree node now partitions space by the lower/upper level sets of a randomly drawn $f \in \mathcal{F} \subset \{g : \mathbb{R}^d \to \mathbb{R}\}$ and a random threshold τ . Selecting \mathcal{F} recovers classic IF (coordinate indicators), Extended IF (linear), Hypersphere IF (radial), Deep-IF (neural), and other proposals, unifying them under a single framework. FuBIFFI then decomposes each anomaly score into per-function, and hence per-feature, contributions by tracing forest path lengths, delivering model-agnostic attributions with a clear probabilistic meaning.

This lens clarifies prior "function-based IF" work, exposes their common principles, and through FuBIFFI, links *detection* directly to *explanation*, enabling actionable insight for practitioners and regulators (Doshi-Velez and Kim, 2017; Rudin, 2019; Arrieta et al., 2020).

The outline of the article: Section 2 reviews the IF and its derivatives. Section 3 explains the FuBIF and FuBIFFI interpretability framework. Section 4 demonstrates the efficacy of FuBIF, comparing it with existing and novel IF-based models. Section 5, with conclusions in Section 6.

2. RELATED WORKS

The Isolation Forest (IF) algorithm (Liu et al., 2008) is a widely used AD method. IF isolates anomalies near the tree root due to fewer splits, but is biased toward data distributed orthogonally to axes, reducing effectiveness in complex datasets. The Extended Isolation Forest

^{*} This work was partially supported by: (1) Regione Veneto Project 'Sistemi Umano centrici per Prodotti e pRocEssi Manufatturieri Evoluti' (SUPREME), PR Veneto FESR 2021–2027. Azione 1.1.1 Sub A. 'Bando per il finanziamento di progetti di ricerca e sviluppo realizzati dalle Reti Innovative Regionali e dai Distretti Industriali' DGR n. 729 of June 26, 2024; (2) MICS (Made in Italy—Circular and Sustainable) Extended Partnership and received funding from Next-GenerationEU (Italian PNRR—M4C2, Invest 1.3—D.D. 1551.11–10–2022, PE00000004); (3) PNRR research activities of the consortium iNEST (Interconnected North-Est Innovation Ecosystem) funded by the European Union Next-GenerationEU (Piano Nazionale di Ripresa e Resilienza (PNRR)—Missione 4 Componente 2, Investimento 1.5—D.D. 1058 23/06/2022, ECS000000043).

(EIF) (Hariri et al., 2019) uses random hyperplanes instead of axis-aligned cuts, reducing orientation bias, but introducing other complexities. The Generalized Isolation Forest (GIF) (Lesouple et al., 2021) improves hyperplane selection by balancing the cut distribution throughout the data range. EIF⁺ (Arcudi et al., 2023) refines threshold selection using normal distribution sampling, reducing bias. The Hypersphere Isolation Forest (HIF) (Choudhury et al., 2021) uses hyperspheres for space partitioning, better capturing certain data structures. The deep isolation forest (DIF) (Xu et al., 2022) utilizes neural networks to transform the data space before applying isolation forest techniques.

Key differences in tree construction and splitting criteria, that FuBIF aims to unify within a single framework, are summarized below.

For **IF** and **EIF**, the criteria is $\mathbf{v} \cdot \mathbf{x} - \tau \leq 0$, where \mathbf{v} is a random unit vector and τ is chosen from the range of projected data; in **IF**, the vector is parallel to the features. A similar rule applies to \mathbf{EIF}^+ , but in this case, τ is sampled from a normal distribution. In **HIF**, the branching function becomes $\|\mathbf{x} - \mathbf{c}\|^2 - R^2 \leq 0$. For **DIF**, the function is $(NN_{\Theta}(\mathbf{x}))_i - \tau \leq 0$, where NN_{Θ} is a randomly initialized neural network.

3. FUNCTION BASED ISOLATION FOREST (FUBIF)

3.1 Isolation based Anomaly Detection

Isolation-based Anomaly Detection models assume abnormal samples are easier to isolate than normal ones. These methods use an ensemble of trees $\mathcal{T} = \{T_1, T_2, \ldots, T_N\}$, trained on a random subsample Y_i drawn from a dataset $X \subset \mathbb{R}^d$. Tree nodes correspond to recursive random splits of data Y_i . Anomalies tend to be isolated near the root, requiring fewer splits. The number of splits required to isolate a sample \mathbf{x} is called its path length, denoted $h_{T_i}(\mathbf{x})$. The Isolation Forest (IF) algorithm and its variants define the anomaly score $s(\mathbf{x},n)$ based on the expected path length across all trees in the forest, normalized by a factor c(n), where n is the subsample size and c(n) is a normalizing factor:

$$s(\mathbf{x}, n) = 2^{\frac{-\mathbb{E}_{T_i \in \mathcal{T}}[h_{T_i}(\mathbf{x})]}{c(n)}}.$$

3.2 Function-based Isolation Forest framework

FuBIF is a generalized mathematical framework for IF models, so a class of algorithms constructed from:

- a set $\mathcal{F} \subset \{f : \mathbb{R}^n \to \mathbb{R}\}$ of data splitting functions,
- sampling distribution ρ over \mathcal{F} ,
- sampling distribution μ over \mathbb{R} for thresholds.

FuBIF preserves forest-structure principles from 3.1, modifying tree ramification. For a sub-sample Y of dataset $X \subset \mathbb{R}^d$, a function f is selected from \mathcal{F} via distribution ρ . A threshold τ is drawn from distribution μ , re-centered by f's sample distribution: $\{f(\mathbf{x})|\mathbf{x}\in Y\}$.

The tree construction process starts with the root node function: $F(\mathbf{x}) = f(\mathbf{x}) - m$, and then the set Y is divided into two subsets:

$$L = \{ \mathbf{x} \in Y \mid F(\mathbf{x}) \le 0 \}, \quad R = \{ \mathbf{x} \in Y \mid F(\mathbf{x}) > 0 \}.$$

This process recursively creates left (L) and right (R) child-nodes until reaching maximum iterations or subset of single point. A FuBIF-tree forest is built from random dataset sub-samples, with anomaly scores determined by average point height. The centering of μ relative to the output of f in FuBIF-tree construction indicates μ 's dependence on f and Y. Function-based algorithms can allow μ , ρ , and $\mathcal F$ to depend on node dataset, tree depth, and previous functions. However, in this paper, $\mathcal F$ is fixed, and ρ is uniform over $\mathcal F$ or re-centered uniform over a subset. Distribution μ types are listed below, where Y is the node subset and f is the chosen function.

Uniform Distribution over the range of f(x) values:

$$\mathcal{U}\left(\left[\min_{\mathbf{x}\in Y} f(\mathbf{x}), \max_{\mathbf{x}\in Y} f(\mathbf{x})\right]\right)$$

Normal Distribution mean/std of f(x) scaled by η :

$$\mathcal{N}\Big(mean\big(\{f(\mathbf{x})|\mathbf{x}\in Y\}\big), \eta std\big(\{f(\mathbf{x})|\mathbf{x}\in Y\}\big)\Big)$$

Substantial differences arise from distribution choice for the domain for splits: one splits within data range, the other extends beyond the range based on η . We denote each algorithm by its triple as (\mathcal{F}, ρ, μ) -IF.

3.3 Tested Examples

This study explores generalizations of the FuBIF algorithm with splitting functions \mathcal{F} as n-dimensional conic sections. Choudhury et al. (2021) explored this with the HIF algorithm using hypersphere level-sets. Table 1 lists splitting function \mathcal{F} , parameter distribution ρ , and threshold distribution μ (defined in 3.2).

Table 1. FuBIF framing of different splitting functions.

Algorithm	Function	Parameters	Tresh.
IF	$f_i(\mathbf{x}) = x_i$	$i \sim U(\{1, \cdots n\})$	unif
EIF	$f_{\mathbf{v}}(\mathbf{x}) = \mathbf{v} \cdot \mathbf{x}$	$\mathbf{v} \sim \mathcal{U}(S^{n-1})$	unif
EIF ⁺	$f_{\mathbf{v}}(\mathbf{x}) = \mathbf{v} \cdot \mathbf{x}$	$\mathbf{v} \sim \mathcal{U}(S^{n-1})$	norm
HIF	$f_c(x) = x - c ^2$	$c \sim U(range(Y))$	unif
Ellipse ⁿ -IF	$f_{c_1,c_2}(\mathbf{x}) = \ \mathbf{x} - \mathbf{c}_1\ + \ \mathbf{x} - \mathbf{c}_2\ $	$c_1, c_2 \sim \mathcal{U}(\mathbf{range}(Y))$	both
Hyper ⁿ -IF	$f_{c_1,c_2}(\mathbf{x}) = \ \mathbf{x} - \mathbf{c}_1\ - \ \mathbf{x} - \mathbf{c}_2\ $	$c_1, c_2 \sim \mathcal{U}(\mathbf{range}(Y))$	both
Para ⁿ -IF	$f_{c,v}(\mathbf{x}) = \mathbf{x} - \mathbf{c} + \mathbf{v} \cdot \mathbf{x}$	$c \sim U(range(Y)), v \sim U(S^{n-1})$	both
$Quad(\lambda)$ -IF	$f_{A,\mathbf{v}}(\mathbf{x}) = \mathbf{x} \cdot (A + A^t)\mathbf{x} + \mathbf{v} \cdot \mathbf{x}$	$A_{ij} \sim \mathcal{N}(0, 1), v_i \sim \mathcal{U}([-\lambda, \lambda])$	both
NN-IF	$f_{\Theta,b}(\mathbf{x}) = NN_{\Theta,b}(\mathbf{x})$	$\Theta \sim \mathcal{N}(0, 1), b \sim \mathcal{U}([-1, 1])$	both

Let n be the ambient space dimension, Y a set of points split at each node, and $\mathbf{range}(Y)$ the hyper-rectangle enveloping Y, defined as:

$$\left[\min_{y\in Y}y_1, \ \max_{y\in Y}y_1\right]\times\cdots\times\left[\min_{y\in Y}y_n, \ \max_{y\in Y}y_n\right].$$

The first four algorithms are well-known, reformulated in the FuBIF framework, while the last five are novel:

- Ellipseⁿ-IF: n-dimensional ellipsoid. For n=2, it's an ellipse; for n=3, an ellipsoid of revolution. The equation $f_{c_1,c_2}(\mathbf{x}) \tau = 0$ describes the locus of points such that the sum of the distances to the foci is constant.
- **Hyper**ⁿ**-IF**: n-dimensional hyperbola branch. For n=2, it's a hyperbola; for n=3, a sheet of a hyperboloid of revolution. The equation $f_{c_1,c_2}(\mathbf{x}) \tau = 0$ describes the locus of points such that the difference (with sign) of the distances from c_1 and c_2 is constant.

- Paraⁿ-IF: n-dimensional paraboloid. Parabola for n=2; a paraboloid of revolution for n=3. The equation $f_{c,v}(\mathbf{x}) \tau = 0$ describes the locus of points such that the distance from focus c equals the distance from the hyperplane $\mathbf{v} \cdot \mathbf{x} \tau = 0$.
- **Quad**(λ)-**IF**: A quadric in n dimensions described by $f_{A,\mathbf{v}}(\mathbf{x}) = \mathbf{x} \cdot (A + A^t)\mathbf{x} + \mathbf{v} \tau = 0$. The matrix A is drawn from $\mathcal{N}(0,1)$, and \mathbf{v} 's entries are drawn from $\mathcal{U}([-\lambda,\lambda])$.
- NN-IF: A random neural network function with scalar output. Given random weights $\Theta \sim \mathcal{N}(0,1)$ and bias $\mathbf{b} \sim \mathcal{U}(-1,1)$, the zero locus is defined by $NN_{\Theta,b}(\mathbf{x}) \tau = 0$.

3.4 Motivation

The main hypothesis is that normal data can be locally modeled as level sets of a function $f(\mathbf{x}) \in \mathcal{F}$.

If dataset $X \subset \mathbb{R}^2$ lies on the sine function graph, the optimal \mathcal{F} would contain $f(x_1,x_2)=x_2-\sin(x_1)$. While this FuBIF effectively finds points deviating from the sine graph, it performs poorly on other structures. Figure 1 shows how $f(x_1,x_2)=x_2-\sin(x_1)$ adapts to the point manifold. This suggests that expanding the set of splitting functions without a balanced probability distribution is not an effective strategy for improving performance and may introduce undesirable biases.

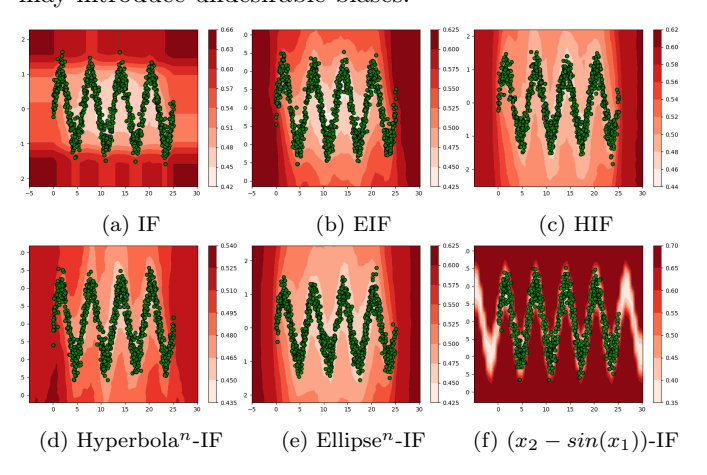


Fig. 1. Anomaly scoremaps generated by different IF-based models, where darker colors indicate more anomalous regions.

Dataset manifold information is often unavailable, requiring $\mathcal F$ to cover various distributions without biases. Literature led to the EIF algorithm addressing IF's coordinate axes bias. While defining biases in FuBIF is challenging, AD should remain invariant to transformations such as translations and rotations. IF's limitations stem from lack of rotational invariance, while Quadric(1)-IF lacks translational invariance. Figure 2 shows that low λ values produce lower scores near the axis center.

3.5 Function-based Isolation Forest Feature Importance.

FuBIF Feature Importance (FuBIFFI), inspired by DIFFI Carletti et al. (2023) and ExIFFI (Arcudi et al., 2023), aims to detect the more relevant features for anomaly detection when any (\mathcal{F}, ρ, μ) -IF is applied.

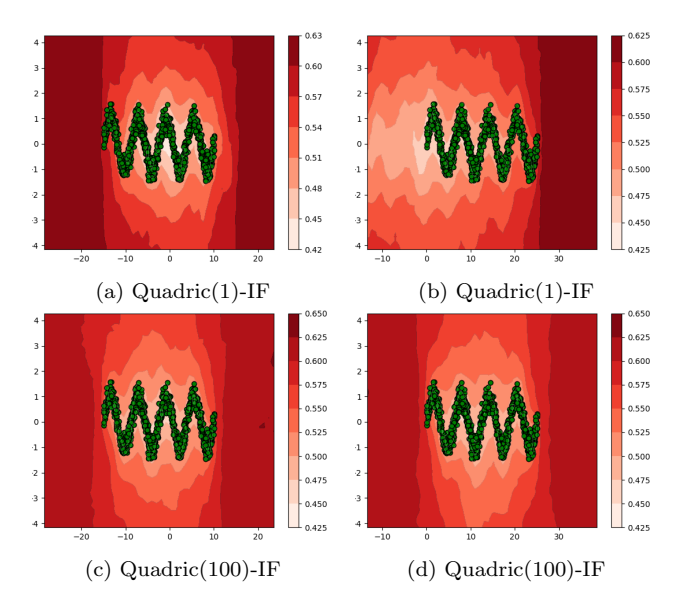


Fig. 2. The images show anomaly scoremaps generated by $\operatorname{Quadric}(\lambda)$ -IF models for $\lambda=1$ and $\lambda=100$. The right column displays the dataset translated left by 10 units with highlighted bias.

Consider a node k in a tree T where a function $f \in \mathcal{F}$ is chosen. The probability of a point \mathbf{x} being in the right child node depends on the threshold τ through the distribution μ . This probability is

$$p_f(\mathbf{x}) := \mathbb{P}_{\mu} \big(\tau \le f(\mathbf{x}) \big) = \int_{-\infty}^{f(\mathbf{x})} \mu'(t) \mathrm{d}t.$$

where μ' is the probability density function of μ . The gradient of this function expresses the rate of change of its probability lying in the right child node of k. It is computed as:

$$\nabla p_f(\mathbf{x}) = \mu'(f(\mathbf{x}))(\partial_1 f(\mathbf{x}), \dots, \partial_n f(\mathbf{x})).$$

To represent the percentage influence of each feature on the probability $p_f(\mathbf{x})$, we square all entries and divide by the norm squared:

$$i_k(\mathbf{x}) = \frac{1}{\|\nabla f(\mathbf{x})\|^2} \Big(\partial_1 f(\mathbf{x})^2, \dots, \partial_n f(\mathbf{x})^2 \Big)$$

If f is linear, as in IF or EIF, ∇f is constant and represents the coordinate vector of the selected feature or vector orthogonal to the splitting hyperplane. In these cases, $i_k(\mathbf{x})$ is independent of \mathbf{x} . Otherwise, $i_k(\mathbf{x})$ is an n-valued function of \mathbf{x} . FuBIFFI uses $i_k(\mathbf{x})$ to produce, for every tree T in the forest, at each node k in the path $\mathcal{P}_T(\mathbf{x})$, a constant vector with positive coordinates summing to 1, representing the relative importance of each feature in the splitting at node k. This vector is defined as:

$$\mathbf{i}_{\mathbf{x}}^k = \frac{1}{|Y_{k+1}|} \sum_{\mathbf{y} \in Y_{k+1}} i_k(\mathbf{y})$$

where Y_{k+1} is the set of points in the next node of $\mathcal{P}_T(\mathbf{x})$. To evaluate feature importance on the whole path $\mathcal{P}_T(\mathbf{x})$, vectors $\mathbf{i}_{\mathbf{x}}^k$ are summed with weights $\lambda_{\mathbf{x}}^k$, emphasizing nodes that effectively isolate \mathbf{x} :

$$\lambda_{\mathbf{x}}^k = \frac{|Y_k|}{|Y_{k+1}| + 1},$$

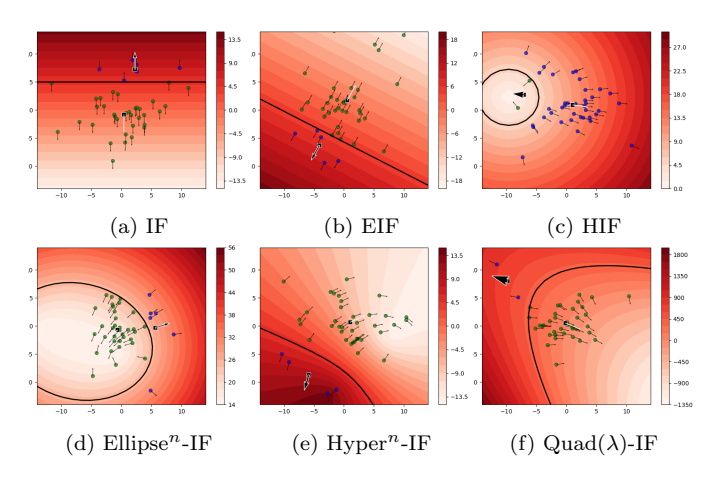


Fig. 3. The images show imbalance projections from a branching function toward the mean direction of two subsets. The color map indicates function score, with the black line marking the threshold. Green and blue points represent the subsets and their derivative directions. The thick black arrow shows the mean derivative direction, its thickness reflecting the imbalance in each subset.

Define

$$\mathbf{i}_{\mathbf{x}}^T = \frac{1}{|\mathcal{P}_T(\mathbf{x})|} \sum_{k \in \mathcal{P}_T(\mathbf{x})} \lambda_{\mathbf{x}}^k \ \mathbf{i}_{\mathbf{x}}^k.$$

This is the vector of feature importance of \mathbf{x} w.r.t. tree T. Define

$$\mathbf{I}_{\mathbf{x}} = \frac{1}{|\mathcal{T}|} \sum_{T \in \mathcal{T}} \mathbf{i}_{\mathbf{x}}^{T}.$$

where \mathcal{T} is the whole forest. This is the vector of local feature importance of \mathbf{x} . The importance score of a feature is its corresponding coordinate in $\mathbf{I}_{\mathbf{x}}$. To evaluate overall feature importance, the dataset is divided into inliers I and outliers O. Define:

$$\mathbf{I}_I = \frac{1}{|I|} \sum_{\mathbf{x} \in I} \mathbf{I}_{\mathbf{x}}, \quad \mathbf{I}_O = \frac{1}{|O|} \sum_{\mathbf{x} \in O} \mathbf{I}_{\mathbf{x}}.$$

The global feature importance vector is the component-wise ratio of I_O and I_I :

$$GFI = \frac{\mathbf{I}_O}{\mathbf{I}_I}$$

The importance score of a feature is its corresponding coordinate in GFI, representing its relevance in separating inliers from outliers. Figure 3 shows the splitting functions and derivative directions, demonstrating how FuBIFFI works.

4. EXPERIMENTS

This section evaluates various FuBIF models from Table 1 and established models from pyod library (Zhao et al., 2019), including IForest (Liu et al., 2008), EIF (Hariri et al., 2019)), HIF (Choudhury et al., 2021), DIF (Xu et al., 2022), and AutoEncoder (AE) (Aggarwal, 2016). These models are tested on benchmark datasets for unsupervised AD, comparing anomaly scores with ground truth.

FuBIFFI reliability is assessed using Feature Selection as a proxy task; and we provide its time complexity analysis.

We also examine NN-IF, whose splitting function is a randomly initialized NN (see Table 1).

4.1 Dataset

We use AD tabular datasets from the "ODDS" library (Rayana, 2016), which contains real-world AD datasets derived from multi-class datasets where the least represented class becomes an outlier, with others merged as inlier class. The datasets appear in Table 2.

Synthetic datasets Xaxis and Bisect_3d are also used. Both are based on a 6-dimensional hypersphere centered at zero, with anomalies along the first feature and the first three features respectively, demonstrating bias in certain splitting functions like IF.

Table 2. Experimental datasets overview.

	data	anomalies	contam features		Size	Type
	n		%	d		
Xaxis	1100	100	9.09	6	(Low)	Synt
Bisec3D	1100	100	9.09	6	(Low)	Synt
Annthyroid	7200	534	7.56	6	(Low)	Real
Breastw	683	239	52.56	9	(Middle)	Real
Cardio	1831	176	9.60	21	(High)	Real
Glass	214	29	13.55	9	(Middle)	Real
Ionosphere	351	126	35.71	33	(High)	Real
Pendigits	6870	156	2.27	16	(Middle)	Real
Pima	768	268	34.89	8	(Middle)	Real
Wine	129	10	7.75	13	(Middle)	Real

4.2 Methodology

Inspired by Pang et al. (2019); Xu et al. (2022), we observed that model performance varies with contamination levels in training data. For real datasets, higher contamination causes IF-based models to include anomalies into the inlier distribution, misclassifying peripheral points as outliers.

Models were evaluated in two training scenarios: **Scenario** I, where all data, including anomalies, were used; and **Scenario** II, where only inliers were used for training.

Two threshold strategies for the splitting function (Section 3.2) were also tested. The \mathcal{U} distribution restricts cuts within the data range; \mathcal{N} permits extrapolated cuts, potentially forming empty branches and improving the detection of unseen anomalies.

Performance was measured via average precision (Avg Prec) and ROC AUC, independent of contamination. Precision based on known contamination was also reported. Since IF-based models are stochastic, in Figure 4 we show an average of 10 runs.

Avg Precision evaluates positive prediction quality by combining precision and recall across thresholds. ROC AUC measures class discrimination ability across thresholds, showing the difference between precise anomaly detection and overall discrimination.

To evaluate the interpretation algorithms, we used the AUC_{FS} metric by Turbé et al. (2023) and refined by Arcudi et al. (2023) for Feature Importance in EIF. This metric measures the area between feature selection processes by comparing the effect of dropping the least versus most important features, and assesses the robustness and reliability in evaluating feature importance.

4.3 Results

Performance Evaluation Table 3 shows the performance metrics of the models from Section 4 on the datasets in Scenario II, where the threshold τ is selected using the normal distribution \mathcal{N} . The average performance across

Table 3. Avg precision results of the models in Scenario 2 with Normal threshold distribution

Dataset	IF	EIF	HIF	Ellipse-IF	Para-IF	Hyper-IF	Quad-IF	NN-IF	DIF	AE
Xaxis	0.06	1.00	1.00	1.00	1.00	1.00	1.00	1.00	1.00	1.00
bisect_3d	1.00	1.00	1.00	1.00	1.00	1.00	1.00	1.00	1.00	1.00
annthyroid	0.47	0.48	0.52	0.52	0.50	0.44	0.48	0.49	0.31	0.44
breastw	0.99	0.99	0.99	0.99	0.99	0.99	0.99	0.96	0.94	0.99
cardio	0.67	0.77	0.76	0.77	0.77	0.64	0.77	0.32	0.79	0.76
glass	0.82	0.77	0.88	0.90	0.85	0.71	0.68	0.67	0.71	0.58
ionosphere	0.92	0.97	0.96	0.95	0.97	0.96	0.96	0.94	0.93	0.87
pendigits	0.47	0.39	0.32	0.29	0.37	0.25	0.37	0.02	0.41	0.24
pima	0.64	0.60	0.61	0.62	0.61	0.57	0.59	0.55	0.56	0.52
wine	0.76	0.85	0.81	0.81	0.86	0.69	0.86	0.67	0.82	0.48
Mean	0.68	0.78	0.79	0.79	0.79	0.73	0.79	0.71	0.76	0.73

all IF-based models is similar, with effectiveness varying by dataset. Based on results we provide in our open-source repository, FuBIF algorithms outperform both AE and DIF models, except for the glass and cardio datasets, even if no branching function consistently outperformed the rest. IF is 1.5 times more effective than Ellipse-IF on the pendigits dataset because of its square-shaped distribution. In contrast, Ellipse-IF performs better in the wine and Xaxis datasets, where the data have a globular distribution. This suggests that branching function selection should be dataset-specific for optimal results.

Interpretability Evaluation The evaluation of the interpretation algorithm shown in Figure 4 demonstrates, through the feature selection performance (AUC_{FS} score), that it remains consistent across models, with some notable exceptions, indicating a need for refinement. The models show varying efficiencies in determining feature importance across datasets, with notable differences between glass and wine.

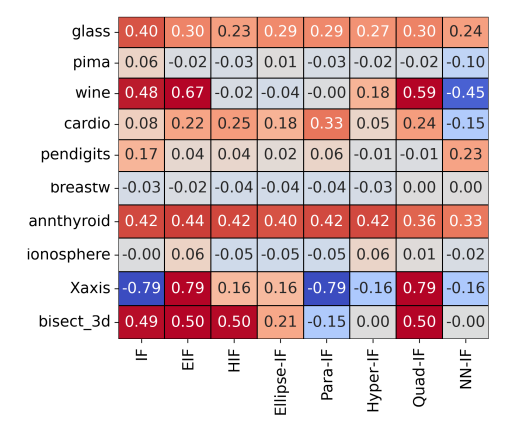


Fig. 4. Heatmap of AUC_{FS} scores for datasets in Scenario II with normal threshold distribution. Higher score indicates better feature selection.

The results show that although no branching function is universally superior, the interpretation algorithm consistently performs feature selection across models and datasets. This robustness demonstrates its effectiveness in identifying the key features and their importance. This insight helps guide branching function selection, align the model structure with domain knowledge, and ensure logical and practical relevance.

4.4 Computational Time Analysis

In Figure 5 we analyze the time complexity of the FuBIF models compared to other algorithms. All FuBIF algorithms show similar time complexity, with slight increases when more parameters are required for branching. FuBIF models' fitting time scales better than AutoEncoder and DIF, although prediction time exceeds DIF. Function-based branching maintains an efficient computation and minimal memory requirements.

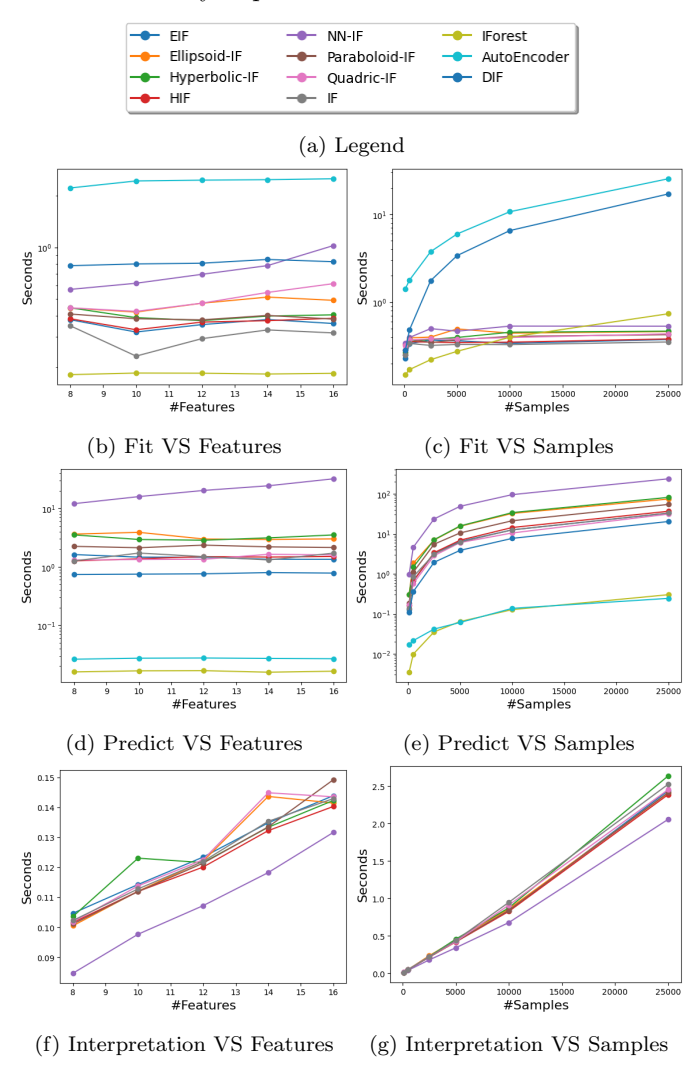
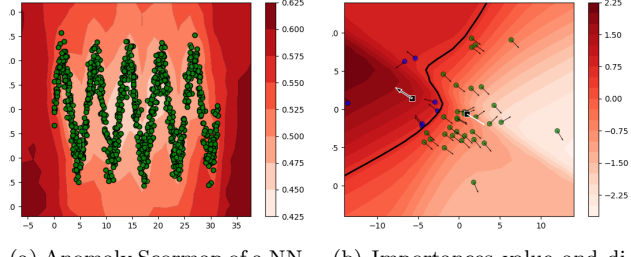


Fig. 5. Computational time of the models varying the size and dimensionality of the dataset.

4.5 Neural Network Branching

Inspired by Xu et al. (2022), we use a randomly initialized Neural Network (NN) as each node's branching function. Unlike DIF, our approach assigns a unique NN per node that maps the dataset to a one-dimensional distribution to generate a branching threshold.

The adaptability of the model is evident in Figure 6a, where the importance directions of the cuts in Figure 6b



- (a) Anomaly Scormap of a NN-IF model
- (b) Importances value and direction of a NN branch

Fig. 6. Analysis of NN branching function

are aligned with the dataset distribution and branching function. However, because of the complexity of neural networks and chaotic gradients, the results are less interpretable than those of other models, as shown by the lower AUC_{FS} scores in Figure 4.

5. FUTURE WORKS

FuBIF unified framework for isolation-based AD algorithms offers improved capabilities while introducing some mathematical complexities. Key research directions include the following.

Bias in Algorithms: Figure 2 shows Quadric(1)-IF's lack of translational invariance, while IF's lack of rotational invariance led to EIF. Research should define biases and develop symmetrization techniques.

Adaptive FuBIF: Future work should develop methods for selecting f from \mathcal{F} , including adapting \mathcal{F} to data subsets.

Ensemble Methods: Using varied branching functions in FuBIF ensembles could improve dataset manifold understanding.

6. CONCLUSION

FuBIF is a unified framework for isolation-based AD, which is generalized and flexible. Its mathematical core and adaptability make it a powerful tool for unsupervised anomaly detection, handling complex data, and offering valuable interpretations. With diverse branching and thresholding functions, FuBIF addresses limitations in traditional Isolation Forest models with promising results; although its effectiveness varies with data characteristics, showing no universally superior branching function. FuBIFFI embeds interpretability by providing a generalized derivation of the feature importance scores for isolation-based algorithms. Research directions include mitigating bias, developing distribution-specific models, and evaluating branching functions.

REFERENCES

Aggarwal, C.C. (2016). Outlier analysis second edition. Arcudi, A., Frizzo, D., Masiero, C., and Susto, G.A. (2023). Exiffi and eif+: Interpretability and enhanced generalizability to extend the extended isolation forest. arXiv preprint arXiv:2310.05468.

Arrieta, A.B., Díaz-Rodríguez, N., Del Ser, J., Bennetot, A., Tabik, S., et al. (2020). Explainable artificial intelligence (xai): Concepts, taxonomies, opportunities and challenges toward responsible ai. *Information fusion*, 58, 82–115.

Carletti, M., Terzi, M., and Susto, G.A. (2023). Interpretable anomaly detection with diffi: Depth-based feature importance of isolation forest. *Eng. Applications of A.I.*, 119, 105730.

Choudhury, J., Ky, P., Ren, Y., and Shi, C. (2021). Hypersphere for branching node for the family of isolation forest algorithms. In 2021 IEEE Int. Conf. on Smart Computing (SMARTCOMP), 418–423. IEEE.

Doshi-Velez, F. and Kim, B. (2017). Towards a rigorous science of interpretable machine learning. arXiv preprint arXiv:1702.08608.

Hariri, S., Kind, M.C., and Brunner, R.J. (2019). Extended isolation forest. *IEEE Tran. on knowledge and data Eng.*, 33(4), 1479–1489.

Kabir, S., Shufian, A., and Zishan, M.S.R. (2023). Isolation forest based anomaly detection and fault localization for solar pv system. In 2023 3rd Int. Con. on Robotics, Electrical and Signal Processing Techniques (ICREST), 341–345. IEEE.

Lesouple, J., Baudoin, C., Spigai, M., and Tourneret, J.Y. (2021). Generalized isolation forest for anomaly detection. *Pattern Recognition Letters*, 149, 109–119.

Liu, F.T., Ting, K.M., and Zhou, Z.H. (2008). Isolation forest. In 2008 eighth IEEE Int. Conf. on data mining, 413–422. IEEE.

Ounacer, S., El Bour, H.A., Oubrahim, Y., Ghoumari, M.Y., and Azzouazi, M. (2018). Using isolation forest in anomaly detection: the case of credit card transactions. *Periodicals of Eng. and Natural Sciences*, 6(2), 394–400.

Pang, G., Shen, C., and Van Den Hengel, A. (2019). Deep anomaly detection with deviation networks. In Proceedings of the 25th ACM SIGKDD international conference on knowledge discovery & data mining, 353–362.

Rayana, S. (2016). ODDS library. URL https://odds.cs.stonybrook.edu.

Rudin, C. (2019). Stop explaining black box machine learning models for high stakes decisions and use interpretable models instead. *Nature machine intelligence*, 1(5), 206–215.

Turbé, H., Bjelogrlic, M., Lovis, C., and Mengaldo, G. (2023). Evaluation of post-hoc interpretability methods in time-series classification. Nature Machine Intelligence, 5(3), 250–260.

Wu, W. and Chen, Y. (2018). Application of isolation forest to extract multivariate anomalies from geochemical exploration data. *Global Geology*, 21(1), 36–47.

Xu, H., Pang, G., Wang, Y., and Wang, Y. (2022). Deep isolation forest for anomaly detection. *IEEE Tran. on Knowledge and Data Eng.*, 35, 12591–12604.

Zhao, Y., Nasrullah, Z., and Li, Z. (2019). Pyod: A python toolbox for scalable outlier detection. *Journal of Machine Learning Research*, 20(96), 1-7. URL http://jmlr.org/papers/v20/19-011.html.